Towards Feedback Control of Compressible Flows Using Galerkin Reduced Order Models

Irina Kalashnikova[1] and Srinivasan Arunajatesan[2]

[1] Numerical Analysis & Applications Department, Sandia National Laboratories*, Albuquerque, NM, U.S.A.
[2] Aerosciences Department, Sandia National Laboratories*, Albuquerque, NM, U.S.A.

Second International Workshop on Model Reduction for Parametrized Systems (MoRePaS II)
Gunzburg, Germany
October 2-5, 2012

* Sandia is a multiprogram laboratory operated by Sandia Corporation, a Lockheed Martin Company, for the United States Department of Energy under Contract DE-AC04-94AL85000.

Outline

Motivation for Numerical Analysis of ROMs

Use of ROMs in predictive applications raises questions about their stability & convergence.

- Projection ROM approach is an alternative discretization of the governing PDEs.
- Desired numerical properties of a ROM discretization:
  - **Consistency** (with continuous PDEs): loosely speaking, a ROM **CAN** be consistent with respect to the full simulations used to generate it.
  - **Stability**: numerical stability is **NOT** in general guaranteed *a priori* for a ROM!
  - **Convergence**: requires consistency and stability.

Motivation for Numerical Analysis of ROMs

Use of ROMs in predictive applications raises questions about their stability & convergence.

- Projection ROM approach is an alternative discretization of the governing PDEs.
- Desired numerical properties of a ROM discretization:
  - **Consistency** (with continuous PDEs): loosely speaking, a ROM **CAN** be consistent with respect to the full simulations used to generate it.
  - **Stability**: numerical stability is **NOT** in general guaranteed *a priori* for a ROM!
  - **Convergence**: requires consistency and stability.

This talk focuses on how to construct a Galerkin ROM that is **stable** *a priori*

Sandia National Laboratories

Model Reduction Approach

High-Fidelity CFD Simulations:

Snapshot 1

Snapshot 2

⋮

Snapshot K

Step 1 →

Fluid Modal Decomposition (POD):

$$\boxed{\mathbf{u}_M = \sum_{k=1}^{M} a_k(t)\boldsymbol{\phi}_k(\mathbf{x})}$$

Step 2 →

Galerkin Projection of Fluid PDEs:

$$\boxed{(\boldsymbol{\phi}_j, \dot{\mathbf{u}}_M + \nabla \cdot \mathbf{F}(\mathbf{u}_M)) = 0}$$

“Small” ROM ODE System:

$$\boxed{\dot{a}_k = f(a_1, \ldots, a_M)}$$

Sandia National Laboratories

Step 1: Constructing the Modes

High-Fidelity
CFD Simulations:

Snapshot 1
Snapshot 2
⋮
Snapshot K

Step 1

Fluid Modal
Decomposition
(POD):

$$\mathbf{u}_M = \sum_{k=1}^{M} a_k(t)\boldsymbol{\phi}_k(\mathbf{x})$$

Step 2

Galerkin Projection
of Fluid PDEs:

$$(\phi_j, \dot{\mathbf{u}}_M + \nabla \cdot \mathbf{F}(\mathbf{u}_M)) = 0$$

"Small"
ROM
ODE
System:

$$\dot{a}_k = f(a_1, ..., a_M)$$

- **POD basis** $\{\phi_i\}_{i=1}^{M}$ with $M << K$ maximizes the energy in the projection of snapshots onto span$\{\phi_i\}$.
- **POD eigenvalue problem**:

$$\mathbf{R}\phi = \lambda\phi$$

where $\mathbf{R}\phi \equiv \langle \mathbf{u}^k(\mathbf{u}^k, \phi)\rangle$.

Sandia National Laboratories

Step 2: Galerkin Projection

High-Fidelity CFD Simulations:

Snapshot 1

Snapshot 2

⋮

Snapshot K

Step 1

Fluid Modal Decomposition (POD):

$$\mathbf{u}_M = \sum_{k=1}^{M} a_k(t)\boldsymbol{\phi}_k(\mathbf{x})$$

Step 2

Galerkin Projection of Fluid PDEs:

$$\boxed{(\boldsymbol{\phi}_j, \dot{\mathbf{u}}_M + \nabla \cdot \mathbf{F}(\mathbf{u}_M)) = 0}$$

"Small" ROM ODE System:

$$\boxed{\dot{a}_k = f(a_1, \ldots, a_M)}$$

- Galerkin projection of ***continuous*** equations in ***continuous*** inner product onto reduced basis modes $\{\boldsymbol{\phi}_i\}_{i=1}^{M}$.

Sandia National Laboratories

Stability Definitions

- **Practical Definition:** Numerical solution does not “blow up” in finite time.

Stability Definitions

- **Practical Definition:** Numerical solution does not “blow up” in finite time.
- **More Precise Definition:** Numerical discretization does not introduce any spurious instabilities inconsistent with natural instability modes supported by the governing continuous PDEs.

Stability Definitions

- **Practical Definition:** Numerical solution does not “blow up” in finite time.
- **More Precise Definition:** Numerical discretization does not introduce any spurious instabilities inconsistent with natural instability modes supported by the governing continuous PDEs.

Numerical solutions **must** maintain a proper energy balance

Stability Definitions

- **Practical Definition:** Numerical solution does not "blow up" in finite time.
- **More Precise Definition:** Numerical discretization does not introduce any spurious instabilities inconsistent with natural instability modes supported by the governing continuous PDEs.

Numerical solutions **must** maintain a proper energy balance

Linearized Compressible Navier-Stokes Equations:
$\frac{dE}{dt} \leq 0$
Non-increasing energy [5]

$\longleftarrow$ duality $\longrightarrow$

Compressible Navier-Stokes Equations:
$\frac{d}{dt}\int_\Omega \rho\eta d\Omega \geq 0$
Clausius-Duhem Inequality
Non-decreasing entropy [4]

Stability Definitions

- **Practical Definition:** Numerical solution does not "blow up" in finite time.
- **More Precise Definition:** Numerical discretization does not introduce any spurious instabilities inconsistent with natural instability modes supported by the governing continuous PDEs.

Numerical solutions **must** maintain a proper energy balance

Linearized Compressible Navier-Stokes Equations:

$$\frac{dE}{dt} \leq 0$$

Non-increasing energy [5]

$\longleftarrow$ duality $\longrightarrow$

Compressible Navier-Stokes Equations:

$$\frac{d}{dt}\int_{\Omega} \rho \eta d\Omega \geq 0$$

Clausius-Duhem Inequality

Non-decreasing entropy [4]

- Analyzed using the **Energy Method**: Uses an equation for the evolution of numerical solution "energy" (or "entropy") to determine stability.

Sandia National Laboratories

3D Linearized Compressible Navier-Stokes Equations

- Appropriate when a compressible fluid system can be described by viscous, small-amplitude perturbations about a steady-state mean (or base) flow.
- Linearization of full compressible Navier-Stokes equations:

$$\mathbf{q}^T(\mathbf{x},t) \equiv \begin{pmatrix} u_1, & u_2, & u_3, & T, & \rho \end{pmatrix} \equiv \underbrace{\bar{\mathbf{q}}^T(\mathbf{x})}_{\text{mean}} + \underbrace{\mathbf{q}'^T(\mathbf{x},t)}_{\text{fluctuation}} \in \mathbb{R}^5$$

$$\boxed{\Rightarrow \mathbf{q}'_{,t} + \mathbf{A}_i \mathbf{q}'_{,i} - [\mathbf{K}_{ij}\mathbf{q}'_{,j}]_{,i} = \mathbf{0}}$$

where

$$\mathbf{A}_1 = \begin{pmatrix} \bar{u}_1 & 0 & 0 & R & \frac{R\bar{T}}{\bar{\rho}} \\ 0 & \bar{u}_1 & 0 & 0 & 0 \\ 0 & 0 & \bar{u}_1 & 0 & 0 \\ \bar{T}(\gamma-1) & 0 & 0 & \bar{u}_1 & 0 \\ \bar{\rho} & 0 & 0 & 0 & \bar{u}_1 \end{pmatrix}, \quad \mathbf{A}_2 = \begin{pmatrix} \bar{u}_2 & 0 & 0 & 0 & 0 \\ 0 & \bar{u}_2 & 0 & R & \frac{R\bar{T}}{\bar{\rho}} \\ 0 & 0 & \bar{u}_2 & 0 & 0 \\ 0 & \bar{T}(\gamma-1) & 0 & \bar{u}_2 & 0 \\ 0 & \bar{\rho} & 0 & 0 & \bar{u}_2 \end{pmatrix}$$

$$\mathbf{A}_3 = \begin{pmatrix} \bar{u}_3 & 0 & 0 & 0 & 0 \\ 0 & \bar{u}_3 & 0 & 0 & 0 \\ 0 & 0 & \bar{u}_3 & R & \frac{R\bar{T}}{\bar{\rho}} \\ 0 & 0 & \bar{T}(\gamma-1) & \bar{u}_3 & 0 \\ 0 & 0 & \bar{\rho} & 0 & \bar{u}_3 \end{pmatrix}, \quad \mathbf{K}_{11} \equiv \frac{1}{\bar{\rho}} \begin{pmatrix} 2\mu+\lambda & 0 & 0 & 0 & 0 \\ 0 & \mu & 0 & 0 & 0 \\ 0 & 0 & \mu & 0 & 0 \\ 0 & 0 & 0 & \frac{(\gamma-1)\kappa}{R} & 0 \\ 0 & 0 & 0 & 0 & 0 \end{pmatrix}, \quad \ldots$$

Sandia National Laboratories

Symmetrized Linearized Compressible Navier-Stokes Equations

Energy stability of the Galerkin ROM can be proven [1] following "symmetrization" the linearized compressible Navier-Stokes equations.

- Linearized compressible Navier-Stokes system is "symmetrizable" [5].
- Pre-multiply equations by symmetric positive definite matrix:

$$\mathbf{H} \equiv \begin{pmatrix} \bar{\rho} & 0 & 0 & 0 & 0 \\ 0 & \bar{\rho} & 0 & 0 & 0 \\ 0 & 0 & \rho & 0 & 0 \\ 0 & 0 & 0 & \frac{\bar{\rho}R}{\bar{T}(\gamma-1)} & 0 \\ 0 & 0 & 0 & 0 & \frac{R\bar{T}}{\bar{\rho}} \end{pmatrix}. \quad \Rightarrow \quad \boxed{\mathbf{H}\mathbf{q}'_{,t} + \mathbf{H}\mathbf{A}_i\,\mathbf{q}'_{,i} - \mathbf{H}[\mathbf{K}_{ij}\mathbf{q}'_{,i}]_{,j} = \mathbf{0}}$$

- $\mathbf{H}$ is called the "symmetrizer" of the system:
  - The convective flux matrices $\mathbf{H}\mathbf{A}_i$ are all symmetric.
  - The following augmented viscosity matrix

$$\mathbf{K}^S \equiv \begin{pmatrix} \mathbf{H}\mathbf{K}_{11} & \mathbf{H}\mathbf{K}_{12} & \mathbf{H}\mathbf{K}_{13} \\ \mathbf{H}\mathbf{K}_{21} & \mathbf{H}\mathbf{K}_{22} & \mathbf{H}\mathbf{K}_{23} \\ \mathbf{H}\mathbf{K}_{31} & \mathbf{H}\mathbf{K}_{32} & \mathbf{H}\mathbf{K}_{33} \end{pmatrix},$$

  is symmetric positive semi-definite.

Sandia National Laboratories

Symmetry Inner Product & A Stable Galerkin ROM

- Define the "symmetry" inner product and "symmetry" norm:

$$(\mathbf{q}'^{(1)}, \mathbf{q}'^{(2)})_{(\mathbf{H},\Omega)} \equiv \int_{\Omega} [\mathbf{q}'^{(1)}]^T \mathbf{H} \mathbf{q}'^{(2)} d\Omega, \qquad ||\mathbf{q}'||_{(\mathbf{H},\Omega)} \equiv (\mathbf{q}', \mathbf{q}')_{(\mathbf{H},\Omega)} \tag{1}$$

Symmetry Inner Product & A Stable Galerkin ROM

- Define the “symmetry” inner product and “symmetry” norm:

$$(\mathbf{q}'^{(1)}, \mathbf{q}'^{(2)})_{(\mathbf{H},\Omega)} \equiv \int_{\Omega} [\mathbf{q}'^{(1)}]^T \mathbf{H} \mathbf{q}'^{(2)} d\Omega, \qquad ||\mathbf{q}'||_{(\mathbf{H},\Omega)} \equiv (\mathbf{q}', \mathbf{q}')_{(\mathbf{H},\Omega)} \tag{1}$$

- Stability analysis reveals that the symmetry inner product (and *not* the L^2 inner product!) is the energy inner product for this equation set.

Sandia National Laboratories

Symmetry Inner Product & A Stable Galerkin ROM

- Define the "symmetry" inner product and "symmetry" norm:

$$(\mathbf{q}'^{(1)}, \mathbf{q}'^{(2)})_{(\mathbf{H},\Omega)} \equiv \int_{\Omega} [\mathbf{q}'^{(1)}]^T \mathbf{H} \mathbf{q}'^{(2)} d\Omega, \qquad ||\mathbf{q}'||_{(\mathbf{H},\Omega)} \equiv (\mathbf{q}', \mathbf{q}')_{(\mathbf{H},\Omega)} \tag{1}$$

- Stability analysis reveals that the symmetry inner product (and *not* the L^2 inner product!) is the energy inner product for this equation set.
- Galerkin approximation $\mathbf{q}'_M = \sum_{i=1}^{M} a_k(t)\phi_k(\mathbf{x})$ satisfies the same energy expression as the solutions to the continuous equations:

$$\boxed{||\mathbf{q}'_M(\mathbf{x},t)||_{(\mathbf{H},\Omega)} \leq e^{\beta t}||\mathbf{q}'_M(\mathbf{x},0)||_{(\mathbf{H},\Omega)}}$$

where β is an upper bound on the eigenvalues of the matrix $\mathbf{B} \equiv \mathbf{H}^{-T/2}\frac{\partial(\mathbf{H}\mathbf{A}_i)}{\partial x_i}\mathbf{H}^{-1/2}$.

Sandia National Laboratories

Symmetry Inner Product & A Stable Galerkin ROM

- Define the "symmetry" inner product and "symmetry" norm:

$$(\mathbf{q}'^{(1)}, \mathbf{q}'^{(2)})_{(\mathbf{H},\Omega)} \equiv \int_\Omega [\mathbf{q}'^{(1)}]^T \mathbf{H}\mathbf{q}'^{(2)} d\Omega, \qquad ||\mathbf{q}'||_{(\mathbf{H},\Omega)} \equiv (\mathbf{q}', \mathbf{q}')_{(\mathbf{H},\Omega)} \qquad (1)$$

- Stability analysis reveals that the symmetry inner product (and *not* the L^2 inner product!) is the energy inner product for this equation set.
- Galerkin approximation $\mathbf{q}'_M = \sum_{i=1}^{M} a_k(t)\phi_k(\mathbf{x})$ satisfies the same energy expression as the solutions to the continuous equations:

$$||\mathbf{q}'_M(\mathbf{x}, t)||_{(\mathbf{H},\Omega)} \leq e^{\beta t} ||\mathbf{q}'_M(\mathbf{x}, 0)||_{(\mathbf{H},\Omega)}$$

where β is an upper bound on the eigenvalues of the matrix $\mathbf{B} \equiv \mathbf{H}^{-T/2} \frac{\partial(\mathbf{H}\mathbf{A}_i)}{\partial x_i} \mathbf{H}^{-1/2}$.

Practical Implication:
Symmetry inner product ensures Galerkin projection step of the ROM is stable for **any** basis!

Steps to Obtain a Stable Compressible Fluid Galerkin ROM

- Galerkin-project the equations in the symmetry inner product (2):

$$\left(\boldsymbol{\phi}_k, \frac{\partial \mathbf{q}'_M}{\partial t}\right)_{(\mathbf{H},\Omega)} + \left(\boldsymbol{\phi}_k, \mathbf{A}_i \frac{\partial \mathbf{q}'_M}{\partial x_i}\right)_{(\mathbf{H},\Omega)} + \left(\boldsymbol{\phi}_k, \frac{\partial}{\partial x_j}\left[\mathbf{K}_{ij}\frac{\partial \mathbf{q}'_M}{\partial x_i}\right]\right)_{(\mathbf{H},\Omega)} = 0 \quad (2)$$

Sandia National Laboratories

Steps to Obtain a Stable Compressible Fluid Galerkin ROM

- Galerkin-project the equations in the symmetry inner product (2):

$$\left(\boldsymbol{\phi}_k, \frac{\partial \mathbf{q}'_M}{\partial t}\right)_{(\mathbf{H},\Omega)} + \left(\boldsymbol{\phi}_k, \mathbf{A}_i \frac{\partial \mathbf{q}'_M}{\partial x_i}\right)_{(\mathbf{H},\Omega)} + \left(\boldsymbol{\phi}_k, \frac{\partial}{\partial x_j}\left[\mathbf{K}_{ij}\frac{\partial \mathbf{q}'_M}{\partial x_i}\right]\right)_{(\mathbf{H},\Omega)} = 0 \quad (2)$$

- Integrate viscous term in (2) by parts and apply boundary conditions:

$$\left(\boldsymbol{\phi}_k, \frac{\partial \mathbf{q}'_M}{\partial t}\right)_{(\mathbf{H},\Omega)} = \int_\Omega \left[\boldsymbol{\phi}_k^T \mathbf{H}\mathbf{A}_i \mathbf{q}'_{M,i} - \boldsymbol{\phi}_{k,j}^T \mathbf{H}\mathbf{K}_{ij}\mathbf{q}'_{M,i}\right] d\Omega - \int_{\partial\Omega} \boldsymbol{\phi}_k^T \mathbf{H}\mathbf{K}_{ij} n_j \, \mathbf{q}'_{M,i} \, dS$$

Insert boundary conditions into boundary integrals (weak implementation)

* Energy stability is maintained if the boundary conditions are such that $\int_{\partial\Omega} \boldsymbol{\phi}_k^T \mathbf{H}\mathbf{K}_{ij} n_j \mathbf{q}'_{M,i} dS \geq 0$.

Steps to Obtain a Stable Compressible Fluid Galerkin ROM

- Galerkin-project the equations in the symmetry inner product (2):

$$\left(\boldsymbol{\phi}_k, \frac{\partial \mathbf{q}'_M}{\partial t}\right)_{(\mathbf{H},\Omega)} + \left(\boldsymbol{\phi}_k, \mathbf{A}_i \frac{\partial \mathbf{q}'_M}{\partial x_i}\right)_{(\mathbf{H},\Omega)} + \left(\boldsymbol{\phi}_k, \frac{\partial}{\partial x_j}\left[\mathbf{K}_{ij}\frac{\partial \mathbf{q}'_M}{\partial x_i}\right]\right)_{(\mathbf{H},\Omega)} = 0 \quad (2)$$

- Integrate viscous term in (2) by parts and apply boundary conditions:

$$\left(\boldsymbol{\phi}_k, \frac{\partial \mathbf{q}'_M}{\partial t}\right)_{(\mathbf{H},\Omega)} = \int_\Omega \left[\boldsymbol{\phi}_k^T \mathbf{H}\mathbf{A}_i \mathbf{q}'_{M,i} - \boldsymbol{\phi}_{k,j}^T \mathbf{H}\mathbf{K}_{ij}\mathbf{q}'_{M,i}\right] d\Omega - \int_{\partial\Omega} \boldsymbol{\phi}_k^T \mathbf{H}\mathbf{K}_{ij} n_j \mathbf{q}'_{M,i} \, dS$$

Insert boundary conditions into boundary integrals (weak implementation)

* Energy stability is maintained if the boundary conditions are such that $\int_{\partial\Omega} \boldsymbol{\phi}_k^T \mathbf{H}\mathbf{K}_{ij} n_j \mathbf{q}'_{M,i} dS \geq 0$.

- Substitute modal decomposition $\mathbf{q}'_M = \sum_k a_k(t)\boldsymbol{\phi}_k(\mathbf{x})$ to obtain an $M \times M$ linear dynamical system of the form $\dot{\mathbf{a}} = \mathbf{C}\mathbf{a}$

3D Full (Non-Linear) Compressible Navier-Stokes Equations

- 3D compressible Navier-Stokes equations:

$$
\begin{aligned}
\rho \frac{Du_1}{dt} &= -\frac{\partial p}{\partial x_1} + \sum_{j=1}^{3} \frac{\partial}{\partial x_j}\left\{\mu\left(\frac{\partial u_1}{\partial x_j} + \frac{\partial u_j}{\partial x_1}\right) + \lambda \delta_{1j} \nabla \cdot \mathbf{u}\right\}, \\
\rho \frac{Du_2}{dt} &= -\frac{\partial p}{\partial x_2} + \sum_{j=1}^{3} \frac{\partial}{\partial x_j}\left\{\mu\left(\frac{\partial u_2}{\partial x_j} + \frac{\partial u_j}{\partial x_2}\right) + \lambda \delta_{2j} \nabla \cdot \mathbf{u}\right\}, \\
\rho \frac{Du_3}{dt} &= -\frac{\partial p}{\partial x_3} + \sum_{j=1}^{3} \frac{\partial}{\partial x_j}\left\{\mu\left(\frac{\partial u_3}{\partial x_j} + \frac{\partial u_j}{\partial x_3}\right) + \lambda \delta_{3j} \nabla \cdot \mathbf{u}\right\}, \\
\rho C_v \frac{DT}{dt} &= -p \nabla \cdot \mathbf{u} + \sum_{i=1}^{3} \frac{\partial}{\partial x_i}\left(\kappa \frac{\partial T}{\partial x_i}\right), \\
\frac{D\rho}{\partial t} &= -\rho \nabla \cdot \mathbf{u}.
\end{aligned}
\tag{3}
$$

- ROM approach is based on local linearization of full non-linear equations (3):
  - Full non-linear equations (3) are solved to generate snapshots in high-fidelity code
  - In the ROM projection step, the equations (3) are linearized around a steady base flow and projected onto the POD modes

3D Full (Non-Linear) Compressible Navier-Stokes Equations

- 3D compressible Navier-Stokes equations:

$$
\begin{aligned}
\rho \frac{Du_1}{dt} &= -\frac{\partial p}{\partial x_1} + \sum_{j=1}^{3} \frac{\partial}{\partial x_j}\left\{\mu\left(\frac{\partial u_1}{\partial x_j} + \frac{\partial u_j}{\partial x_1}\right) + \lambda \delta_{1j} \nabla \cdot \mathbf{u}\right\}, \\
\rho \frac{Du_2}{dt} &= -\frac{\partial p}{\partial x_2} + \sum_{j=1}^{3} \frac{\partial}{\partial x_j}\left\{\mu\left(\frac{\partial u_2}{\partial x_j} + \frac{\partial u_j}{\partial x_2}\right) + \lambda \delta_{2j} \nabla \cdot \mathbf{u}\right\}, \\
\rho \frac{Du_3}{dt} &= -\frac{\partial p}{\partial x_3} + \sum_{j=1}^{3} \frac{\partial}{\partial x_j}\left\{\mu\left(\frac{\partial u_3}{\partial x_j} + \frac{\partial u_j}{\partial x_3}\right) + \lambda \delta_{3j} \nabla \cdot \mathbf{u}\right\}, \\
\rho C_v \frac{DT}{dt} &= -p \nabla \cdot \mathbf{u} + \sum_{i=1}^{3} \frac{\partial}{\partial x_i}\left(\kappa \frac{\partial T}{\partial x_i}\right), \\
\frac{D\rho}{\partial t} &= -\rho \nabla \cdot \mathbf{u}.
\end{aligned}
\qquad (3)
$$

- ROM approach is based on local linearization of full non-linear equations (3):
  - Full non-linear equations (3) are solved to generate snapshots in high-fidelity code

    $\Rightarrow$ non-linear dynamics *are* captured in POD modes.

  - In the ROM projection step, the equations (3) are linearized around a steady base flow and projected onto the POD modes

    $\Rightarrow$ non-linear dynamics are *not* captured in ROM equations.

Sandia National Laboratories

Implementation

- **Stability-Preserving Discrete Implementation of ROM:**
  - ROM is implemented in a C++ code that uses distributed vector and matrix data structures and parallel eigensolvers from the `Trilinos` project [7].
  - POD modes defined using piecewise smooth finite elements.
  - Gauss quadrature rules of sufficient accuracy are used to compute exactly inner products with the help of `libmesh` library.

ROM code is potentially compatible with any CFD code that can output a mesh and snapshot data stored at the nodes of this mesh.

- **High-fidelity CFD Code: SIGMA CFD**
  - Sandia in-house finite volume flow solver derived from LESLIE3D [8], a LES flow solver originally developed in the Computational Combustion Laboratory at Georgia Tech.
  - Solves the turbulent compressible flow equations using an explicit 2-4 MacCormack scheme.
  - A hybrid scheme coupling the MacCormack scheme to flux difference splitting schemes is employed to capture shocks.

Inviscid Pulse in a Uniform Base Flow

- Uniform base flow:

$$\begin{aligned}\bar{p} &= 101,325 \text{ Pa}\\ \bar{T} &= 300 \text{ K}\\ \bar{\rho} &= \frac{\bar{p}}{R\bar{T}} = 1.17 \text{ kg/m}^3\\ \bar{u}_1 = \bar{u}_2 &= \bar{u}_3 = 0.0 \text{ m/s}\\ \bar{c} &= 348.0 \text{ m/s.}\end{aligned}$$

- Domain $\Omega = (-1,1) \times (-1,1) \times (-1,-0.9)$ initialized with pressure pulse:

$$\begin{aligned}p'(\mathbf{x};0) &= 141.9e^{-10(x^2+y^2)},\\ \rho'(\mathbf{x};0) &= \frac{p'(\mathbf{x};0)}{R\bar{T}},\\ T'(\mathbf{x};0) &= 0,\\ u_1'(\mathbf{x};0) = u_2'(\mathbf{x};0) &= u_3'(\mathbf{x};0) = 0.\end{aligned}$$

- Slip wall boundary conditions applied on all 6 boundaries of Ω.
- High-fidelity CFD simulation run on 3362 node mesh until time $T = 0.01$ seconds.
- 200 snapshots (saved every 5×10^{-5} seconds), used to construct 20 mode POD bases.

Time History of ROM Modal Amplitudes

Figure 1: 20 Mode Symmetry ROM

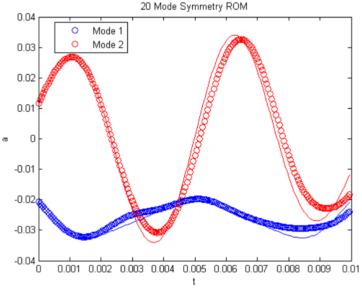

Figure 2: 20 Mode L^2 ROM

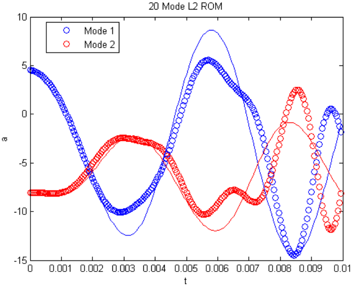

- Figures show:
  - $\circ$: t vs. $a_i(t)$ (ROM coefficients).
  - $-$: t vs. $(\mathbf{q}'_{CFD}(\mathbf{x},t), \boldsymbol{\phi}_i(\mathbf{x}))$ (projection of snapshots onto modes).
- Good agreement between the symmetry ROM and the full simulation for all times.
- Oscillations in the L^2 ROM modal amplitudes observed for $t > 0.008$ seconds suggest the presence of an instability in the L^2 ROM.

20 Mode ROM vs. High-Fidelity Pressure Solutions

Symmetry ROM

L^2 ROM

CFD

Figure 3: Pressure solutions

- Good qualitative agreement between the high-fidelity solution and the symmetry ROM solution.

Laminar Viscous Cavity Problem (Case L2 in [8])

- Free stream pressure = 25 Pa, free stream temperature = 300 K, free stream velocity = 208.8 m/s, $\mu = 1.846 \times 10^{-5}$ kg/(m·s) and $\kappa = 2.587 \times 10^{-2}$ m^2/s.
- Flow initialized to:
  - Zero velocity, free stream pressure, and temperature inside cavity.
  - Free stream conditions, and allowed to evolve, in region above the cavity.

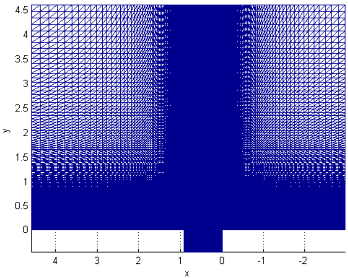

- High-fidelity CFD simulation was run on 343,408 node mesh until time $T = 0.2$ seconds.
- 101 snapshots were saved (every 2×10^{-3} seconds), to construct 30 mode POD bases.

Laminar Viscous Cavity Problem (Case L2 in [8])

- Free stream pressure = 25 Pa, free stream temperature = 300 K, free stream velocity = 208.8 m/s, $\mu = 1.846 \times 10^{-5}$ kg/(m·s) and $\kappa = 2.587 \times 10^{-2}$ m^2/s.
- Flow initialized to:
  - Zero velocity, free stream pressure, and temperature inside cavity.
  - Free stream conditions, and allowed to evolve, in region above the cavity.

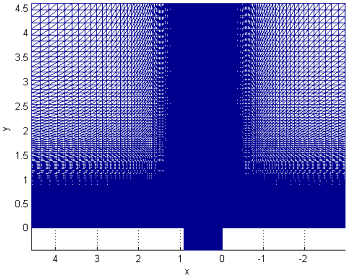

- High-fidelity CFD simulation was run on 343,408 node mesh until time $T = 0.2$ seconds.
- 101 snapshots were saved (every 2×10^{-3} seconds), to construct 30 mode POD bases.

Inherently non-linear problem!
High-fidelity solution obtained by solving full *non-linear* Navier-Stokes equations.

Expected ROM Performance

ROM based on Navier-Stokes equations *linearized* around snapshot mean.

Expected ROM Performance

ROM based on Navier-Stokes equations
linearized around snapshot mean.

Non-linear dynamics of flow
are captured in
POD reduced basis modes.

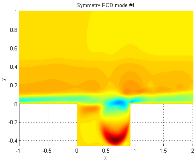

Mode 1 (52.2% energy)

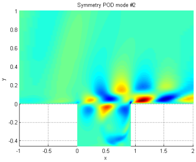

Mode 2 (15.5% energy)

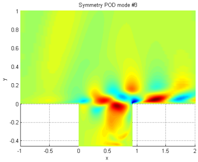

Mode 3 (13.8% energy)

Expected ROM Performance

ROM based on Navier-Stokes equations *linearized* around snapshot mean.

Non-linear dynamics of flow *are* captured in POD reduced basis modes.

Non-linear dynamics of the flow are *not* captured in equations projected onto POD modes.

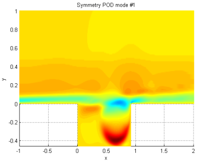

Mode 1 (52.2% energy)

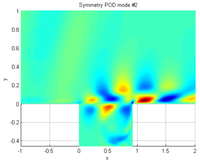

Mode 2 (15.5% energy)

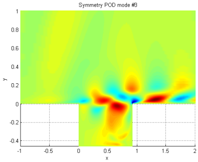

Mode 3 (13.8% energy)

Expected ROM Performance (continued)

- As shear layer separates from the leading edge of the cavity, instabilities develop and grow non-linearly to form vortices convecting down the shear layer.

Expected ROM Performance (continued)

- As shear layer separates from the leading edge of the cavity, instabilities develop and grow non-linearly to form vortices convecting down the shear layer.

ROM built using a linearized form of the Navier-Stokes equations is not be expected to capture accurately this process.

Expected ROM Performance (continued)

- As shear layer separates from the leading edge of the cavity, instabilities develop and grow non-linearly to form vortices convecting down the shear layer.

ROM built using a linearized form of the Navier-Stokes equations is not be expected to capture accurately this process.

- Further downstream, vortices impinge on the aft wall giving rise to linear and non-linear pressure waves that are propagated upstream through the free stream and the cavity.

Expected ROM Performance (continued)

- As shear layer separates from the leading edge of the cavity, instabilities develop and grow non-linearly to form vortices convecting down the shear layer.

ROM built using a linearized form of the Navier-Stokes equations is not be expected to capture accurately this process.

- Further downstream, vortices impinge on the aft wall giving rise to linear and non-linear pressure waves that are propagated upstream through the free stream and the cavity.

The linear waves (expected in this low Re number regime) should be accurately captured by the ROM.

30 Mode ROM vs. High-Fidelity Velocity Solutions

CFD

L^2 ROM

Symmetry ROM

- Reasonable qualitative agreement between ROM and high-fidelity solutions.
- ROMs do not capture in full detail inherently non-linear vortical structures present in the high-fidelity solution.

Stability of 30 Mode ROMs

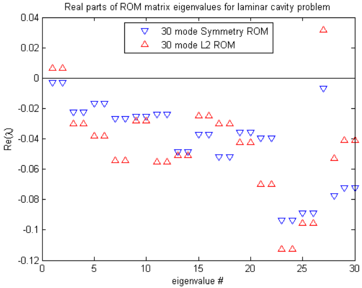

- Figure plots real part of each eigenvalue of the 30×30 ROM dynamical system matrix $\mathbf{C}$ for the 30 mode symmetry and L^2 ROMs.
- 30 mode symmetry ROM is stable, whereas stability of L^2 ROM is not guaranteed.

Target Cavity Flow Control Problem

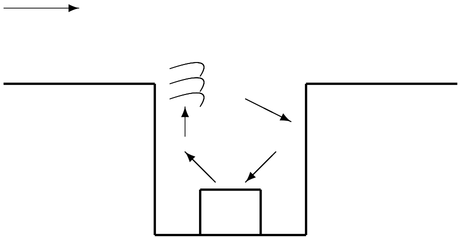

- **Configuration/Plant:** compressible non-linear fluid flow over open cavity containing components.

Target Cavity Flow Control Problem

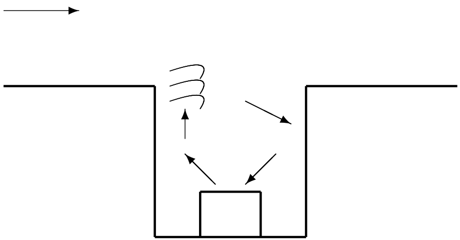

- **Configuration/Plant:** compressible non-linear fluid flow over open cavity containing components.
- **Physical Control Problem:** using upstream actuation, control oscillations within cavity caused by pressure fluctuations propagating between downstream wall and shear layer.

Target Cavity Flow Control Problem

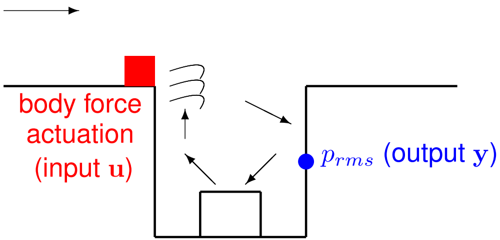

- **Configuration/Plant:** compressible non-linear fluid flow over open cavity containing components.
- **Physical Control Problem:** using upstream actuation, control oscillations within cavity caused by pressure fluctuations propagating between downstream wall and shear layer.
- **Mathematical Control Problem:** compute optimal body-force actuation input $\mathbf{u}_{opt}$ to minimize the RMS pressure halfway up the downstream wall.

$$\text{input } \mathbf{u}: \quad \mathbf{q}^T = \begin{pmatrix} 0, & f(t), & 0 & 0 & 0 \end{pmatrix}^T$$

$$\text{output } \mathbf{y}: \quad p_{rms} = \sqrt{\frac{1}{K}\sum_{i=1}^{K}(p(t_k) - \bar{p})^2}$$

Sandia National Laboratories

Controller Design Options

- **Optimal Controller:** postulates family of desired controls and an objective functional.
  - Requires solution of formal minimization problem involving PDEs and their adjoints.

Non-linear
High-Fidelity CFD

$$\begin{cases} \dot{\mathbf{x}} = \mathbf{f}(\mathbf{x}, \mathbf{u}), \\ \mathbf{y} = \mathbf{h}(\mathbf{x}, \mathbf{u}) \end{cases}$$

Controller Design Options

- **Optimal Controller:** postulates family of desired controls and an objective functional.
  - Requires solution of formal minimization problem involving PDEs and their adjoints.
- **PID Controller:** determines control of the form

$$\mathbf{u}(t) = k_p \mathbf{e}(t) + k_i \int_0^{t_i} \mathbf{e}(\tau) d\tau + k_d \frac{d\mathbf{e}(t)}{dt}$$

from measure of error $\mathbf{e}(t) = \hat{\mathbf{y}}(t) - \mathbf{y}(t)$, where $\hat{\mathbf{y}}(t)$ = desired reference value.

Non-linear
High-Fidelity CFD

$$\begin{cases} \dot{\mathbf{x}} &= \mathbf{f}(\mathbf{x}, \mathbf{u}), \\ \mathbf{y} &= \mathbf{h}(\mathbf{x}, \mathbf{u}) \end{cases}$$

Sandia National Laboratories

Controller Design Options

- **Optimal Controller:** postulates family of desired controls and an objective functional.
  - Requires solution of formal minimization problem involving PDEs and their adjoints.
- **PID Controller:** determines control of the form

$$\mathbf{u}(t) = k_p \mathbf{e}(t) + k_i \int_0^{t_i} \mathbf{e}(\tau) d\tau + k_d \frac{d\mathbf{e}(t)}{dt}$$

  from measure of error $\mathbf{e}(t) = \hat{\mathbf{y}}(t) - \mathbf{y}(t)$, where $\hat{\mathbf{y}}(t)$ = desired reference value.
- **LQG** $(\mathcal{H}_2)$ **Controller:** finds linear control law $\mathbf{u} = -\mathbf{K}\mathbf{x}$ that minimizes the objective function

$$J = \frac{1}{T} \int_0^T (\mathbf{y}^T \mathbf{y} + \mathbf{u}^T \mathbf{R} \mathbf{u}) dt$$

  - Computation of $\mathbf{K} = \mathbf{R}^{-1}\mathbf{B}^T\mathbf{X}$ requires solution of algebraic Ricatti equation $\mathbf{A}^T\mathbf{X} + \mathbf{X}\mathbf{A} - \mathbf{X}\mathbf{B}\mathbf{R}^{-1}\mathbf{B}^T\mathbf{X} + \mathbf{C}^T\mathbf{C} = \mathbf{0}$.

Non-linear
High-Fidelity CFD

$$\begin{cases} \dot{\mathbf{x}} = \mathbf{f}(\mathbf{x}, \mathbf{u}), \\ \mathbf{y} = \mathbf{h}(\mathbf{x}, \mathbf{u}) \end{cases}$$

less expensive

Linearized
High-Fidelity CFD

$$\begin{cases} \dot{\mathbf{x}} = \mathbf{A}\mathbf{x} + \mathbf{B}\mathbf{u}, \\ \mathbf{y} = \mathbf{C}\mathbf{x} + \mathbf{D}\mathbf{u} \end{cases}$$

Controller Design Options

- **Optimal Controller:** postulates family of desired controls and an objective functional.
  - Requires solution of formal minimization problem involving PDEs and their adjoints.
- **PID Controller:** determines control of the form

$$\mathbf{u}(t) = k_p \mathbf{e}(t) + k_i \int_0^{t_i} \mathbf{e}(\tau) d\tau + k_d \frac{d\mathbf{e}(t)}{dt}$$

  from measure of error $\mathbf{e}(t) = \hat{\mathbf{y}}(t) - \mathbf{y}(t)$, where $\hat{\mathbf{y}}(t)$ = desired reference value.
- **LQG** $(\mathcal{H}_2)$ **Controller:** finds linear control law $\mathbf{u} = -\mathbf{K}\mathbf{x}$ that minimizes the objective function

$$J = \frac{1}{T} \int_0^T (\mathbf{y}^T \mathbf{y} + \mathbf{u}^T \mathbf{R} \mathbf{u}) dt$$

  - Computation of $\mathbf{K} = \mathbf{R}^{-1} \mathbf{B}_r^T \mathbf{X}$ requires solution of algebraic Ricatti equation $\mathbf{A}_r^T \mathbf{X} + \mathbf{X}\mathbf{A}_r - \mathbf{X}\mathbf{B}_r \mathbf{R}^{-1} \mathbf{B}_r^T \mathbf{X} + \mathbf{C}_r^T \mathbf{C}_r = \mathbf{0}$.

Non-linear
High-Fidelity CFD

$$\begin{cases} \dot{\mathbf{x}} &= \mathbf{f}(\mathbf{x}, \mathbf{u}), \\ \mathbf{y} &= \mathbf{h}(\mathbf{x}, \mathbf{u}) \end{cases}$$

less expensive ↓

Linearized
High-Fidelity CFD

$$\begin{cases} \dot{\mathbf{x}} &= \mathbf{A}\mathbf{x} + \mathbf{B}\mathbf{u}, \\ \mathbf{y} &= \mathbf{C}\mathbf{x} + \mathbf{D}\mathbf{u} \end{cases}$$

less expensive ↓

Linearized
ROM

$$\begin{cases} \dot{\mathbf{x}}_r &= \mathbf{A}_r \mathbf{x}_r + \mathbf{B}_r \mathbf{u}_r, \\ \mathbf{y}_r &= \mathbf{C}_r \mathbf{x}_r + \mathbf{D}_r \mathbf{u}_r \end{cases}$$

ROM-Based Cavity Flow Control Road Map

1. Collect snapshots from non-linear high-fidelity CFD cavity simulation

$$\dot{\mathbf{x}} = \mathbf{f}(\mathbf{x}, \mathbf{u}_i), \qquad \mathbf{y}_i = \mathbf{h}(\mathbf{x}, \mathbf{u}_i)$$

for some set of inputs $\{\mathbf{u}_i(t)\}$, and construct empirical basis (POD, BPOD) from this snapshot set.

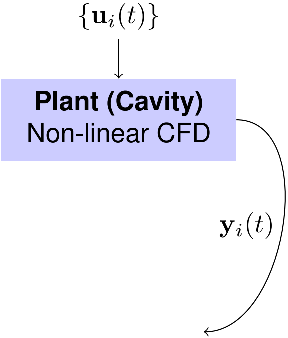

ROM-Based Cavity Flow Control Road Map

1. Collect snapshots from non-linear high-fidelity CFD cavity simulation

$$\dot{\mathbf{x}} = \mathbf{f}(\mathbf{x}, \mathbf{u}_i), \qquad \mathbf{y}_i = \mathbf{h}(\mathbf{x}, \mathbf{u}_i)$$

   for some set of inputs $\{\mathbf{u}_i(t)\}$, and construct empirical basis (POD, BPOD) from this snapshot set.

2. Pick a base flow to linearize around. Build ROM for linearized compressible flow using Galerkin projection in symmetry inner product.

$$\dot{\mathbf{x}}_r = \mathbf{A}_r\mathbf{x}_r + \mathbf{B}_r\mathbf{u}_r, \qquad \mathbf{y}_r = \mathbf{C}_r\mathbf{x}_r + \mathbf{D}_r\mathbf{u}_r$$

$\{\mathbf{u}_i(t)\}$

Plant (Cavity)
Non-linear CFD

$\mathbf{y}_i(t)$

ROM-Based Cavity Flow Control Road Map

1. Collect snapshots from non-linear high-fidelity CFD cavity simulation

$$\dot{\mathbf{x}} = \mathbf{f}(\mathbf{x}, \mathbf{u}_i), \qquad \mathbf{y}_i = \mathbf{h}(\mathbf{x}, \mathbf{u}_i)$$

   for some set of inputs $\{\mathbf{u}_i(t)\}$, and construct empirical basis (POD, BPOD) from this snapshot set.

2. Pick a base flow to linearize around. Build ROM for linearized compressible flow using Galerkin projection in symmetry inner product.

$$\dot{\mathbf{x}}_r = \mathbf{A}_r\mathbf{x}_r + \mathbf{B}_r\mathbf{u}_r, \qquad \mathbf{y}_r = \mathbf{C}_r\mathbf{x}_r + \mathbf{D}_r\mathbf{u}_r$$

3. Compute optimal controller $\mathbf{u}_{opt}(t)$ (estimator/controller) using ROM.

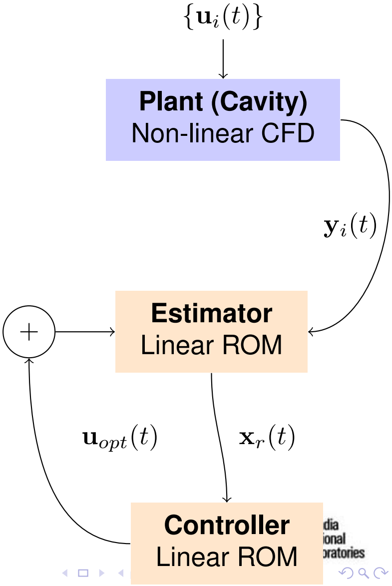

ROM-Based Cavity Flow Control Road Map

1. Collect snapshots from non-linear high-fidelity CFD cavity simulation

$$\dot{\mathbf{x}} = \mathbf{f}(\mathbf{x}, \mathbf{u}_i), \qquad \mathbf{y}_i = \mathbf{h}(\mathbf{x}, \mathbf{u}_i)$$

   for some set of inputs $\{\mathbf{u}_i(t)\}$, and construct empirical basis (POD, BPOD) from this snapshot set.

2. Pick a base flow to linearize around. Build ROM for linearized compressible flow using Galerkin projection in symmetry inner product.

$$\dot{\mathbf{x}}_r = \mathbf{A}_r\mathbf{x}_r + \mathbf{B}_r\mathbf{u}_r, \qquad \mathbf{y}_r = \mathbf{C}_r\mathbf{x}_r + \mathbf{D}_r\mathbf{u}_r$$

3. Compute optimal controller $\mathbf{u}_{opt}(t)$ (estimator/controller) using ROM.
4. Apply ROM-based controller to non-linear cavity problem.

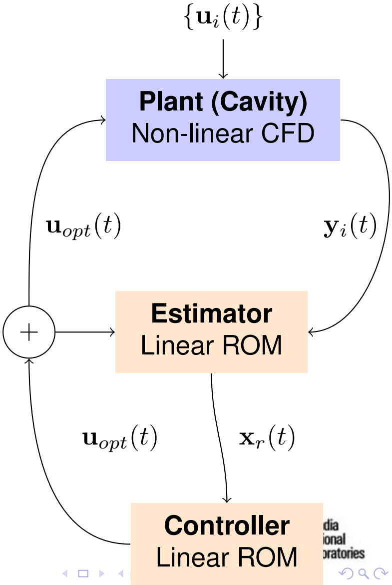

Summary & Future Work

- A Galerkin ROM in which the *continuous* equations are projected onto the basis modes in a *continuous* inner product is proposed.
- The choice of inner product for the Galerkin projection step is crucial to stability of the ROM.
- For linearized compressible flow, Galerkin projection in the "symmetry" inner product leads to a ROM that is stable for any choice of basis.
- Extensions to non-linear compressible flows based on a local linearization of the governing equations prior to projection is described.
- Performance of the proposed POD/Galerkin ROM is examined on a linear as well as a non-linear test case.
- Future work: robust ROM-based control for compressible cavity flows.

Summary & Future Work

- A Galerkin ROM in which the *continuous* equations are projected onto the basis modes in a *continuous* inner product is proposed.
- The choice of inner product for the Galerkin projection step is crucial to stability of the ROM.
- For linearized compressible flow, Galerkin projection in the "symmetry" inner product leads to a ROM that is stable for any choice of basis.
- Extensions to non-linear compressible flows based on a local linearization of the governing equations prior to projection is described.
- Performance of the proposed POD/Galerkin ROM is examined on a linear as well as a non-linear test case.
- Future work: robust ROM-based control for compressible cavity flows.

@ **SIAM CS&E 2013**
"Model Order Reduction of Complex Systems in CFD" Minisymposium
February 25-March 1, 2013
Boston, MA, U.S.A.

References (www.sandia.gov/∼ikalash)

[1] **I. Kalashnikova**, S. Arunajatesan. "A Stable Galerkin Reduced Order Model (ROM) for Compressible Flow". *WCCM Paper No. 2012-18407*, 10th World Congress for Computational Mechanics (WCCM), Sao Paulo, Brazil (July 2012).

[2] **I. Kalashnikova**, M.F. Barone. "On the Stability and Convergence of a Galerkin Reduced Order Model (ROM) of Compressible Flow with Solid Wall and Far-Field Boundary Treatment". *Int. J. Numer. Meth. Engng.* **83** (2010) 1345-1375.

[3] M.F. Barone, **I. Kalashnikova**, D.J. Segalman, H. Thornquist. "Stable Galerkin Reduced Order Models for Linearized Compressible Flow". *J. Comput. Phys.* **288** (2009) 1932-1946.

[4] **I. Kalashnikova**, M.F. Barone. "Stable and Efficient Galerkin Reduced Order Model for Non-Linear Fluid Flow". *AIAA Paper No. 2011–3110, 6th AIAA Theoretical Fluid Mechanics Conference*, Honolulu, HI (June 2011).

[5] J.S. Hesthaven, D. Gottlieb. "A stable penalty method for the compressible Navier-Stokes equations: I. Open boundary conditions." *SIAM J. Sci. Comput.* **17**(3) 579–612 (1996).

[6] V. Sankaran, S. Menon. "LES of Scalar Mixing in Supersonic Shear Layers." *Proceedings of the Combustion Institute*, **30**(2) 2835–2842 (2004).

[7] M.A. Heroux, R.A. Bartlett, V.E. Howle, R.J. Hoekstra, J.J. Hu, T.G. Kolda, R.B. Lehoucq, K.R. Long, R.P. Pawlowski, E.T. Phipps, A.G. Salinger, H.K. Thornquist, R.S. Tuminaro, J.M. Willenbring, A. Williams, K.S. Stanley. "An overview of the Trilinos project". *ACM Trans. Math. Softw.* **31**(3) (2005).

[8] C.W. Rowley, T. Colonius, A.J. Basu. "On self-sustained oscillations in two-dimensional compressible flow over rectangular cavities." *J. Fluid Mech.* **455** 315–346 (2002).

References (www.sandia.gov/∼ikalash)

[1] **I. Kalashnikova**, S. Arunajatesan. "A Stable Galerkin Reduced Order Model (ROM) for Compressible Flow". *WCCM Paper No. 2012-18407*, 10th World Congress for Computational Mechanics (WCCM), Sao Paulo, Brazil (July 2012).

[2] **I. Kalashnikova**, M.F. Barone. "On the Stability and Convergence of a Galerkin Reduced Order Model (ROM) of Compressible Flow with Solid Wall and Far-Field Boundary Treatment". *Int. J. Numer. Meth. Engng.* **83** (2010) 1345-1375.

[3] M.F. Barone, **I. Kalashnikova**, D.J. Segalman, H. Thornquist. "Stable Galerkin Reduced Order Models for Linearized Compressible Flow". *J. Comput. Phys.* **288** (2009) 1932-1946.

[4] **I. Kalashnikova**, M.F. Barone. "Stable and Efficient Galerkin Reduced Order Model for Non-Linear Fluid Flow". *AIAA Paper No. 2011–3110, 6th AIAA Theoretical Fluid Mechanics Conference*, Honolulu, HI (June 2011).

[5] J.S. Hesthaven, D. Gottlieb. "A stable penalty method for the compressible Navier-Stokes equations: I. Open boundary conditions." *SIAM J. Sci. Comput.* **17**(3) 579–612 (1996).

[6] V. Sankaran, S. Menon. "LES of Scalar Mixing in Supersonic Shear Layers." *Proceedings of the Combustion Institute*, **30**(2) 2835–2842 (2004).

[7] M.A. Heroux, R.A. Bartlett, V.E. Howle, R.J. Hoekstra, J.J. Hu, T.G. Kolda, R.B. Lehoucq, K.R. Long, R.P. Pawlowski, E.T. Phipps, A.G. Salinger, H.K. Thornquist, R.S. Tuminaro, J.M. Willenbring, A. Williams, K.S. Stanley. "An overview of the Trilinos project". *ACM Trans. Math. Softw.* **31**(3) (2005).

[8] C.W. Rowley, T. Colonius, A.J. Basu. "On self-sustained oscillations in two-dimensional compressible flow over rectangular cavities." *J. Fluid Mech.* **455** 315–346 (2002).

Thank you! Questions?

ikalash@sandia.gov

Sandia National Laboratories